

## Plant Cell-Wall Cross-Links by REDOR NMR Spectroscopy

Lynette Cegelski,<sup>\*,†,‡</sup> Robert D. O'Connor,<sup>†</sup> Dirk Stueber,<sup>†,¶</sup> Manmilan Singh,<sup>†</sup>  
Barbara Poliks,<sup>§</sup> and Jacob Schaefer<sup>†</sup>

*Department of Chemistry, Washington University, St. Louis, Missouri 63130, United States,  
Department of Chemistry, Stanford University, Stanford, California 94305, United States, and  
Department of Physics, State University of New York at Binghamton, Binghamton,  
New York 13902, United States*

Received June 11, 2010; E-mail: cegelski@stanford.edu

**Abstract:** We present a new method that integrates selective biosynthetic labeling and solid-state NMR detection to identify *in situ* important protein cross-links in plant cell walls. We have labeled soybean cells by growth in media containing L-[ring-*d*<sub>4</sub>]tyrosine and L-[ring-4-<sup>13</sup>C]tyrosine, compared whole-cell and cell-wall <sup>13</sup>C CPMAS spectra, and examined intact cell walls using <sup>13</sup>C{<sup>2</sup>H} rotational echo double-resonance (REDOR) solid-state NMR. The proximity of <sup>13</sup>C and <sup>2</sup>H labels shows that 25% of the tyrosines in soybean cell walls are part of isodityrosine cross-links between protein chains. We also used <sup>15</sup>N{<sup>13</sup>C} REDOR of intact cell walls labeled by L-[ε-<sup>15</sup>N,6-<sup>13</sup>C]lysine and depleted in natural-abundance <sup>15</sup>N to establish that the side chains of lysine are not significantly involved in covalent cross-links to proteins or sugars.

### Introduction

The plant cell wall is a supramolecular, self-assembling, interactive network of structural polysaccharides and glycoproteins, minerals, and water;<sup>1</sup> it is the ultimate biopolymer, able to respond to the functional needs of the organism it protects. The complexity of the plant cell wall is essential for a plant's ability to adapt to differing environmental conditions. However, many structural aspects of the plant cell wall remain elusive, due largely to its insoluble, intractable, and heterogeneous nature. New analytical methods are needed to dissect cell-wall composition and architecture and cell-wall assembly processes.

Macroscopically, a great deal is understood about plant cell-wall composition.<sup>2</sup> Plants assemble a primary cell wall that is tough yet flexible and accommodates cell division and growth. Many cells, particularly those in xylem vessels and woody plants, assemble a secondary cell wall between the cell membrane and the primary cell wall. The secondary cell wall can have a composition that is similar to that of the primary cell wall but often has a high lignin component, which imparts mechanical strength for the entire cell.

The primary cell wall contains four major types of macromolecules: cellulose, hemicellulose, pectins, and proteins.<sup>2</sup> Celluloses consist of linear chains of glucose repeat units, covalently linked by β-1,4-glycosidic bonds.<sup>3</sup> These chains form crystalline microfibrils which aggregate within a matrix of less precisely packed chains of cellulose and hemicellulose, the name given to a heterogeneous group of branched matrix polysaccharides that bind tightly but, for the most part, noncovalently

to the surface of microfibril aggregates and to each other. Pectins, the third major type of cell-wall polysaccharide, are polymers of α-1,4-linked galacturonic acid interspersed with residues of 1,2-linked rhamnose.<sup>4</sup> Divalent cations, particularly Ca<sup>2+</sup>, form complexes with the carboxyl and hydroxyl groups of pectins, resulting in intra- and possibly interchain bridges.<sup>4</sup>

The primary cell wall also contains a proteinaceous structural component. Proteins localized in plant cell walls are unusually rich in one or two amino acids which are present in domains having a highly repetitive sequence. The proteins are generally either highly or poorly glycosylated.<sup>5</sup> The most important classes of cell-wall proteins are the hydroxyproline-rich glycoproteins (HRGPs, sometimes called extensins), the glycine-rich proteins (GRPs), the proline-rich proteins (PRPs), and the arabinogalactan proteins (AGPs).<sup>6–12</sup> There are also lesser concentrations of proteins that have mixtures of the characteristic domains of the four major types.

The HRGPs have the common sequence Ser-Hyp-Hyp-Hyp-Hyp, with most of the hydroxyproline residues glycosylated with tri- and tetra-arabinosides. Interspersed between these HRGP repeats are sequences rich in lysines, histidines, and tyrosines in repetitive motifs. The PRPs have the repeat Pro-Hyp-Val-Tyr-Lys. The GRPs are mostly polyglycine, composed of up to 68% Gly and 12% Ser with some Tyr. The AGPs are 90%

(4) Jarvis, M. C. *Plant, Cell Environ.* **1984**, *7*, 153–164.

(5) Cassab, G. I. *Annu. Rev. Plant Physiol. Plant Mol. Biol.* **1998**, *49*, 281–309.

(6) Showalter, A. M. *Plant Cell* **1993**, *5*, 9–23.

(7) Tierney, M. L.; Varner, J. E. *Plant Physiol.* **1987**, *84*, 1–2.

(8) Keller, B.; Sauer, N.; Lamb, C. J. *EMBO J.* **1988**, *7*, 3625–3633.

(9) Mousavi, A.; Hotta, Y. *Appl. Biochem. Biotechnol.* **2005**, *120*, 169–174.

(10) Marcus, A.; Greenberg, J.; Averyhartfullard, V. *Physiol. Plantarum* **1991**, *81*, 273–279.

(11) Fincher, G. B.; Stone, B. A.; Clarke, A. E. *Annu. Rev. Plant Physiol. Plant Mol. Biol.* **1983**, *34*, 47–70.

(12) Lampport, D. T. A.; Northcote, D. H. *Nature* **1960**, *188*, 665–666.

<sup>†</sup> Washington University.

<sup>‡</sup> Stanford University.

<sup>§</sup> State University of New York at Binghamton.

<sup>¶</sup> Present address: Process Research and Center for Materials Science and Engineering, Merck & Co., Inc., Rahway, NJ 07065.

(1) Varner, J. E.; Lin, L. S. *Cell* **1989**, *56*, 231–239.

(2) Cosgrove, D. J. *Nat. Rev. Mol. Cell. Biol.* **2005**, *6*, 850–861.

(3) O'Sullivan, A. C. *Cellulose* **1997**, *4*, 173–207.

carbohydrate, with the 10% protein component rich in Hyp, Ala, Thr, Gly, and Ser. These proteins exhibit different abundances in the walls of different cell types and are likely to contribute to specific functions.

Formation of an HRGP–cellulose framework seems to be associated with an increase in tensile strength of the cell wall.<sup>13</sup> Carrot root tissues synthesize large quantities of HRGP following wounding and aeration.<sup>14</sup> All of the major cell-wall proteins are insoluble and difficult to extract.<sup>15</sup> Consistent with cell-wall solubilization experiments, it is thought that proteins within the cell wall can participate in aromatic cross-links similar to those of lignin to render the cell wall insoluble.<sup>16</sup> The cross-links could be formed between two amino acids or between protein and one or more of the three types of cell-wall polysaccharides. Tyrosine was proposed as a cross-linking amino acid in plant cell-wall glycoproteins by Fry in 1982 on the basis of results from electrophoresis and thin-layer chromatography of cell-wall hydrolysates that were consistent with the presence of isodityrosine.<sup>16</sup> However, direct detection of isodityrosine or other tyrosine cross-links *in vivo* is challenging due to intrinsic cell-wall insolubility and has not been possible; the putative phenolic protein cross-links are generally attributed to the insoluble and intractable cell-wall constituents that are recalcitrant to digestion during typical sample preparation. Analytically, the direct detection of isodityrosine (and other, more complicated tyrosine–tyrosine cross-links) is possible but requires specialized purification and detection procedures that, in regard to plant cell walls, have been implemented successfully only using simplified samples prepared from purified starting materials that are then exposed to cross-linking conditions *in vitro*, by either chemical or enzyme mediation.<sup>17</sup>

In this study, we have employed solid-state NMR spectroscopy to characterize quantitatively intact cell walls of cultured soybean cells, and we report on the direct detection of isodityrosine cross-links *in situ*. The identification of Tyr–Tyr cross-links relied on <sup>13</sup>C and <sup>2</sup>H labeling with <sup>13</sup>C{<sup>2</sup>H} rotational echo double-resonance (REDOR) NMR detection<sup>18</sup> and was aided by the unique aromatic carbon chemical shifts<sup>19</sup> and <sup>13</sup>C–<sup>2</sup>H dipolar couplings associated with the isodityrosine structure. We also report the absence of any significant concentrations of cross-links involving the side chains of lysine. Our methods combine the strategic implementation of biosynthetic isotope-labeling schemes (using selectively labeled tyrosines and lysines as well as <sup>15</sup>N-depleted ammonium nitrate) with REDOR NMR detection and can be employed in other areas of biology where the characterization of cross-links that involve tyrosine and lysine is of interest.

## Methods

**Maintenance of Plant Cell Culture.** Soybean suspension cultures (cv. Williams 82, a generous gift from Prof. Jack Widholm, Department of Crop Sciences, University of Illinois, Urbana–

Champaign, IL) were grown in 250 mL Erlenmeyer flasks containing 60 mL of cells in Murashige and Skoog's (MS) medium or 1 L flasks containing 250 mL of broth, supplemented with 0.4 mg/L 2,4-dichlorophenoxyacetic acid, at 28 °C with shaking at 120 rpm. MS medium consists of the following on a per liter basis: 1.65 g of NH<sub>4</sub>NO<sub>3</sub>, 1.9 g of KNO<sub>3</sub>, 370 mg of MgSO<sub>4</sub>·7H<sub>2</sub>O, 170 mg of KH<sub>2</sub>PO<sub>4</sub>, 0.83 mg of KI, 6.2 mg of H<sub>3</sub>BO<sub>3</sub>, 22.3 mg of MnSO<sub>4</sub>·4H<sub>2</sub>O, 8.6 mg of ZnSO<sub>4</sub>·7H<sub>2</sub>O, 100 mg of myo-inositol, 440 mg of CaCl<sub>2</sub>·2H<sub>2</sub>O; 27.8 mg of FeSO<sub>4</sub>·7H<sub>2</sub>O, 37.3 mg of Na<sub>2</sub>EDTA·2H<sub>2</sub>O, 0.025 mg of CuSO<sub>4</sub>·5H<sub>2</sub>O, 0.25 mg of Na<sub>2</sub>MoO<sub>4</sub>·2H<sub>2</sub>O, 0.025 mg of CoCl<sub>2</sub>·6H<sub>2</sub>O, 0.50 mg of nicotinic acid, 0.50 mg of pyridoxine-HCl, 0.10 mg of thiamine-HCl, 2.0 mg of glycine, and 30 g of sucrose. Cells were grown for 7–14 days and propagated by transferring 10 mL of suspension growth to 40 mL of MS medium. Longer term cultures were propagated on MS agar medium. Cells depleted in natural-abundance <sup>15</sup>N were grown by substitution of <sup>15</sup>N-depleted ammonium nitrate (HH-2-81-23, Monsanto Research Corp., Mound Facility, Miamisburg, OH) and potassium nitrate (Isotec, Miamisburg, OH) in the MS medium.

**Preparation of Isotopically Labeled Soybean Cells.** Soybean cells were grown in MS medium supplemented with 200 mg/L of each of the desired labeled amino acids. Cells were propagated as above and harvested after different generations to determine the minimum labeling period necessary for maximum label incorporation. Whole cells were harvested by centrifugation at 1000g for 5 min at 4 °C in 50 mL conical tubes. Medium was poured off, and the cells were resuspended in phosphate-buffered saline or water and spun again. Six washes were performed to ensure removal of labeled amino acids in the medium. Whole cells were frozen and lyophilized for NMR sample preparation. Cells were also grown in MS medium supplemented with unlabeled amino acids at the same final concentration for spectral comparisons.

**Cell-Wall Isolation.** Lyophilized whole cells were disrupted by sonication. Approximately 600 mg of lyophilized whole cells (which corresponds to about 10 mL of packed, wet cells) was suspended in 30 mL of homogenization buffer (0.1% potassium acetate, 4 mM Na<sub>2</sub>S<sub>2</sub>O<sub>5</sub>, pH 5.0), kept slowly stirring in an ice–water bath, and sonicated for 10–13 min at 11 V until cell rupture was complete, as monitored by microscopy. Staining with propidium iodide confirmed the removal of DNA/nuclei from the cells. By visual inspection, the cell walls were left almost intact, corresponding to lengths greater than one-half the cell circumference. After sonication, the walls were collected on a Spectra Mesh Nylon filter with a 70 μm pore size and washed with 2 mM Na<sub>2</sub>S<sub>2</sub>O<sub>5</sub>/0.5% IGEPAL CA-630. The detergent was removed by washes with 2 mM Na<sub>2</sub>S<sub>2</sub>O<sub>5</sub>. Finally, the walls were washed several times with water, frozen, and lyophilized. The resulting cell-wall lyophilized powder is white.

**Amino Acid Analyses.** Amino acid analyses of cultured soybean whole cells and isolated cell walls were performed at the Protein and Nucleic Acid Chemistry Laboratory, Washington University School of Medicine.

**Rotational Echo Double-Resonance.** REDOR was used to restore the dipolar couplings between heteronuclear pairs of spins that are removed by magic-angle spinning.<sup>20</sup> REDOR experiments are always done in two parts, once with rotor-synchronized dephasing pulses (*S*) and once without (*S*<sub>0</sub>). The dephasing pulses change the sign of the heteronuclear dipolar coupling, and this interferes with the spatial averaging resulting from the motion of the rotor. The difference in signal intensity ( $\Delta S = S_0 - S$ ) for the observed spin in the two parts of the REDOR experiment, scaled by *S*<sub>0</sub>, is directly related to the corresponding distance to the dephasing spin.

**Spectrometers.** <sup>13</sup>C{<sup>2</sup>H} REDOR NMR was performed using a four-frequency transmission line probe<sup>21</sup> having a 12 mm long, 6 mm inner diameter analytical coil and a Chemagnetics/Varian

- (13) Fry, S. C. *Annu. Rev. Plant Physiol. Plant Mol. Biol.* **1986**, *37*, 165–186.
- (14) Chrispeels, M. J.; Sadava, D.; Cho, Y. P. *J. Exp. Botany* **1974**, *25*, 1157–1166.
- (15) Qi, X. Y.; Behrens, B. X.; West, P. R.; Mort, A. J. *Plant Physiol.* **1995**, *108*, 1691–1701.
- (16) Fry, S. C. *Biochem. J.* **1982**, *204*, 449–455.
- (17) Held, M. A.; Tan, L.; Kamyab, A.; Hare, M.; Shpak, E.; Kieliszewski, M. J. *J. Biol. Chem.* **2004**, *279*, 55474–55482.
- (18) Schmidt, A.; McKay, R. A.; Schaefer, J. J. *Magn. Reson.* **1992**, *96*, 644–650.
- (19) McDowell, L. M.; Burzio, L. A.; Waite, J. H.; Schaefer, J. J. *Biol. Chem.* **1999**, *274*, 20293–20295.

- (20) Gullion, T.; Schaefer, J. J. *Magn. Reson.* **1989**, *81*, 196–200.

**Table 1.** Percent Molar Composition of Amino Acids in Cultured Whole Cells and Cell Walls

amino acid	whole cells	cell walls
alanine	28.6	6.5
glycine	8.1	16.1
hydroxyproline	2.3	7.7
lysine	4.5	6.1
proline	3.2	5.1
tyrosine	5.2	3.5

ceramic stator. Lyophilized samples were contained in thin-wall Chemagnetics/Varian 5 mm outer diameter zirconia rotors. The rotors were spun at 6250 Hz, with the speed under active control to within  $\pm 2$  Hz. A stack-mounted air chiller cooled the rotor to an exit-gas temperature of 10 °C. A 12 T static magnetic field was provided by an 89 mm bore Magnex superconducting solenoid. The spectrometer was controlled by a Tecmag Apollo console. Radiofrequency pulses for  $^2\text{H}$  (76.83 MHz) and  $^{13}\text{C}$  (125.86 MHz) were produced by 2 kW American Microwave Technology power amplifiers under active control. Proton (500.50 MHz) radiofrequency pulses were generated by a 2 kW Amplifier Systems tube amplifier driven by a 50 W American Microwave Technology power amplifier. The  $\pi$ -pulse lengths were 5  $\mu\text{s}$  for  $^2\text{H}$  and  $^{13}\text{C}$ . The  $^{13}\text{C}$  spectra were acquired corresponding to a sweep width of  $\pm 250$  kHz.  $^{13}\text{C}\{^2\text{H}\}$  REDOR spectra were collected with xy-8 phase-cycled  $\pi$  pulses on both the  $^{13}\text{C}$  and  $^2\text{H}$  channels.<sup>22</sup> Proton-carbon cross-polarization (CP) transfers were made in 2 ms with a ramped  $^{13}\text{C}$  radiofrequency field whose nominal average value was 70 kHz. Proton dipolar decoupling was 104 kHz during data acquisition.

The  $^{13}\text{C}\{^{15}\text{N}\}$  REDOR measurements were performed with a six-frequency transmission line probe,<sup>21</sup> 5 mm rotors, 7143 Hz spinning, a 12-T Magnex solenoid, a Tecmag Libra pulse programmer, and power amplifiers similar to those described above.  $^{15}\text{N}\{^{13}\text{C}\}$  REDOR measurements used a four-frequency transmission line probe,<sup>21</sup> 7.5 mm rotors, 5 kHz spinning, a 7 T Oxford solenoid, a Chemagnetics console, and American Microwave Technology power amplifiers. The  $\pi$ -pulse lengths were 10  $\mu\text{s}$  for  $^{13}\text{C}$  and  $^{15}\text{N}$ . Proton decoupling was performed at 100 kHz.

**Molecular Dynamics.** Molecular dynamics simulations were performed using Materials Studio 4.0 software from Accelrys, San Diego, CA. Simulations used the CVFF force field, a time step of 1 fs, and a total time of 100 ps at a temperature of 300 K with frames sampled every 100 fs.

## Results and Discussion

**Whole-Cell and Cell-Wall Composition.** Plant cell walls constitute approximately 20% of the whole-cell mass (dry weight) and exhibit characteristic differences in amino acid composition from whole cells. Standard amino acid analysis of the Williams 82 cultured soybean cells and cell walls used in this study revealed these anticipated attributes (Table 1). Most hydroxyproline residues are in the cell wall. Glycine is more abundant in cell walls, represented in the GRPs, whereas alanine is more prevalent in cytoplasmic proteins.

Global compositional differences were revealed also in the  $^{13}\text{C}$  spectra of labeled whole cells and cell walls (Figure 1). For perspective, the cell-wall spectrum was scaled to represent the contribution of cell walls (by mass) in the whole-cell spectrum. The carbohydrate region (60–90 ppm) dominates the scaled cell-wall spectrum due to high concentrations (ap-

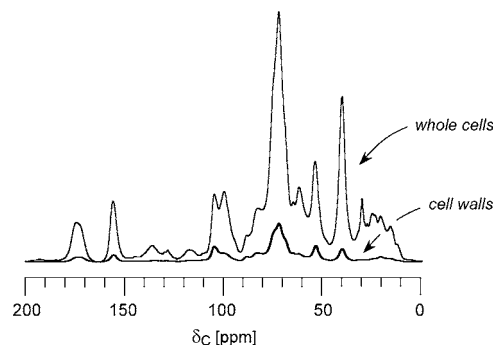


**Figure 1.** 125 MHz  $^{13}\text{C}$  spectral comparison of labeled soybean whole cells (top) and cell walls (bottom). Cells were grown in medium supplemented with 200 mg/L L-[ $\epsilon$ - $^{15}\text{N}$ ,6- $^{13}\text{C}$ ]Lys, L-[ $^{15}\text{N}$ ]Pro, L-[3- $^{13}\text{C}$ ]Ser, L-[ring- $d_4$ ]Tyr, and L-[ring-4- $^{13}\text{C}$ ]Tyr. These are  $S_0$  spectra of 64 $T_r$  (rotor period) REDOR measurements which were acquired using a 2 ms contact time, a 1.5 s recycle delay, and a spinning speed of 7143 Hz. A total of 131 072 scans were acquired for the 200 mg cell-wall sample and 123 360 scans for the 124 mg whole-cell sample. The spectra are scaled by composition.

proximately 20–30% of the total cell-wall mass<sup>1</sup>) of polysaccharides in the cell walls. The cell-wall spectrum has reduced intensity in the aromatic region (110–145 ppm), reflecting the reduced fraction of aromatic amino acids in cell-wall proteins compared to cytoplasmic proteins. Purine carbons in whole cells contribute substantially to the peak at 136 ppm. Their removal during the cell-wall isolation resulted in diminution of this peak in the cell-wall spectrum. Together, the amino acid analysis and NMR spectra confirm the efficacy of the cell-wall preparation. Isolated cell walls rather than whole cells were employed in all measurements to search for cell-wall cross-links to increase NMR sensitivity.

**Direct Detection of Cell-Wall Isodityrosine Cross-Links.**  $^{13}\text{C}\{^2\text{H}\}$  REDOR measurements were performed to identify putative isodityrosine cross-links in isolated soybean cell walls labeled with L-[ring- $^2\text{H}_4$ ]Tyr and L-[ring-4- $^{13}\text{C}$ ]Tyr, hereafter referred to as [ $^2\text{H}$ ]Tyr and [ $^{13}\text{C}$ ]Tyr, respectively. Carbon- and deuterium-labeled tyrosines are assumed to be equally probable, and four types of putative isodityrosine cross-links are possible from the distribution of the two tyrosine labels in proteins. One-fourth of the cross-linked tyrosine pairs would result from two  $^{13}\text{C}$ -labeled tyrosines and one-fourth from a  $^2\text{H}$ -labeled tyrosine pair. These cross-links would not result in  $^{13}\text{C}\{^2\text{H}\}$  dephasing. The remaining one-half of possible cross-links would be formed by a [ $^{13}\text{C}$ ]Tyr-[ $^2\text{H}$ ]Tyr pair. One half of these [ $^{13}\text{C}$ ]Tyr-[ $^2\text{H}$ ]Tyr pairs contribute to the 155 ppm tyrosine peak in the full-echo spectrum (Figure 2, middle, gray). In these pairs, the [ $^{13}\text{C}$ ]Tyr ring is not modified (Figure 2, middle, left inset, red). The other half of the [ $^{13}\text{C}$ ]Tyr-[ $^2\text{H}$ ]Tyr pairs (Figure 2, middle, right inset, blue) contribute to the signature diphenolic peak in the  $^{13}\text{C}$  full-echo spectrum at 145 ppm.<sup>19</sup> That is, the peak observed in the  $^{13}\text{C}$  full-echo spectrum at 145 ppm indicates the presence of an O-linked tyrosyl ring, although the  $^{13}\text{C}$  chemical shift alone does not demonstrate that the moiety O-linked to [ $^{13}\text{C}$ ]Tyr is another tyrosine residue.

$^{13}\text{C}\{^2\text{H}\}$  REDOR was employed to measure the strength of  $^{13}\text{C}$ – $^2\text{H}$  dipolar couplings to make the confirmation. If the 145 ppm carbon were strongly coupled to deuterons, [ $^{13}\text{C}$ ]Tyr with its 145 ppm carbon would necessarily be cross-linked to an O-linked [ $^2\text{H}$ ]Tyr. The observed  $^{13}\text{C}\{^2\text{H}\}$  REDOR dephasing for the 145 ppm peak is 17% at 24 $T_r$  (not shown) and 20% at 48 $T_r$  (Figure 2, second from top), suggesting that a C–D distance of the order of 3 Å is present. For quantification, the

(21) Schaefer, J.; McKay, R. A. Multi-tuned single coil transmission line probe for nuclear magnetic resonance spectrometer. U.S. Patent 5,861,748, 1999.

(22) Gullion, T.; Baker, D. B.; Conradi, M. S. *J. Magn. Reson.* **1990**, *89*, 479–484.



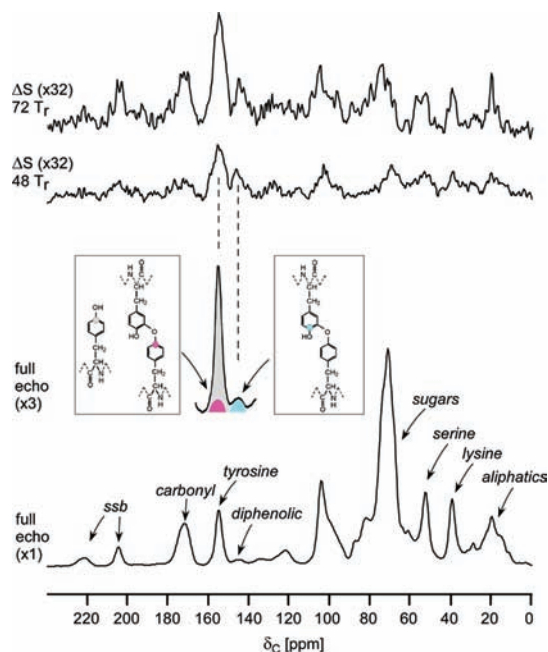


**Figure 2.** Spectral identification and quantification of isodityrosine in cell walls *in situ* by  $^{13}\text{C}\{^2\text{H}\}$  REDOR. Measurements were made on a 500 MHz spectrometer with 96 mg of cell walls labeled with L- $[\epsilon\text{-}^{15}\text{N}, 6\text{-}^{13}\text{C}]\text{Lys}$ , L- $[\text{ring-}d_4\text{-}^{13}\text{C}]\text{Tyr}$ , and L- $[\text{ring-}4\text{-}^{13}\text{C}]\text{Tyr}$ . The insets show possible chemical environments for the tyrosine  $^{13}\text{C}$  labels, color coded by their full-echo chemical-shift assignments. Deuterium tyrosine labels are not shown. The 48 $T_r$  experiment involved the acquisition of 327 680 scans, and the 72 $T_r$  experiment, 262 144 scans. Magic-angle spinning was at 6250 Hz.

observed dephasing is multiplied by a factor of 2 to account for the 50% isotopic dilution of  $[\text{H}]\text{Tyr}$  partners by  $[\text{C}]\text{Tyr}$ . That is, half of the 145 ppm  $[\text{C}]\text{tyrosines}$  are cross-linked to another  $^{13}\text{C}$ -labeled tyrosine and are not influenced by  $^2\text{H}$  REDOR dephasing. The scaled  $^{13}\text{C}\{^2\text{H}\}$  dephasing at 48 $T_r$  is therefore 40%. At 72 $T_r$ , the observed  $^{13}\text{C}\{^2\text{H}\}$  dephasing increases to 30% (Figure 2, top), scaled to 60%, which is nearly complete if we assume that the dephasing is dominated by the single nearest  $^2\text{H}$ . The maximum theoretical dephasing for  $^{13}\text{C}\{^2\text{H}\}$  REDOR is 66% for an isolated  $^{13}\text{C}\text{--}^2\text{H}$  pair.<sup>18</sup> Thus, we conclude that every tyrosine giving rise to the 145 ppm peak is engaged in a cross-link.

**Full-Spectrum REDOR Analysis and Complete Accounting of Tyrosine.** All of the other major  $^{13}\text{C}$  resonances in the full-echo  $S_0$  spectrum are dephased to some extent by deuterated tyrosines (Figure 2). The 175 ppm REDOR difference at the top of Figure 2 shows 1.5% dephasing, which can arise from adventitious placement of  $^2\text{H}$ -labeled rings near peptide carbonyl carbons. The  $\Delta S/S_0$  for lysine (39 ppm) and serine (50 ppm) is 1% each. The large sugar peak at 72 ppm has a  $\Delta S/S_0$  of 0.5%. The  $^2\text{H}$  REDOR dephasing of lysines, serines, and sugars is attributed to incidental contact with  $[\text{H}]\text{Tyr}$ . Notably, the  $^{13}\text{C}\{^2\text{H}\}$   $\Delta S/S_0$  of the 155 ppm tyrosine peak is 3%, which arises from this incidental contact with deuterated tyrosines in cell-wall proteins plus enhanced contact resulting from nearby isodityrosine cross-links (see below).

The percentage of tyrosines that are engaged in cross-links can be determined by comparison of the relative integrated areas of the peaks at 145 and 155 ppm, assuming that CP dynamics and  $T_2$  relaxation are approximately similar for the two. Because both the 145 and 155 ppm peaks arise from nonprotonated ring C-4 carbons, the source of polarization is a transfer from a

collection of nearby protons and will be closely similar for both types of carbons.<sup>23</sup> In addition, these carbons are on the ring  $C_2$  axis and, therefore, are relatively insensitive to local dynamics.<sup>24,25</sup> In addition, no differences were observed in  $S_0 T_2$ 's for the two carbons between 48 and 72 $T_r$ , which supports the validity of comparing the selected carbon peak intensities. The integrated area of the peak centered at 145 ppm is about one-seventh that of the 155 ppm integrated peak area in the full-echo  $S_0$  spectrum (Figure 2, middle, gray and blue). The peak at 155 ppm contains contributions from un-cross-linked tyrosine in proteins (Figure 2, middle, left inset, gray) and from the tyrosine of a cross-linked pair that lacks the diphenolic chemical shift signature. The latter contribution is equal to that of the peak at 145 ppm. Thus, 25% percent  $[(2/7)/(1 + 1/7)]$  of all tyrosines in the cell wall are engaged in isodityrosine cross-links.

**Intrachain vs Interchain Isodityrosine Cross-Links.** The presence of the common YKY sequence motif in HRGPs has inspired a hypothesis that intrachain tyrosine cross-links might be formed by the Tyr<sub>1</sub>-Tyr<sub>3</sub> pair in the motif.<sup>26</sup> Tyr<sub>1</sub>-Tyr<sub>3</sub> homodimers were detected in tryptic digests of isolated extensin. However, this analysis was performed only on the smallest isodityrosine-containing peptide,<sup>27</sup> and absolute quantification was not possible. Analysis of larger peptides might have revealed tyrosine-tyrosine cross-links formed by more sequence-distant tyrosines. Indeed, such cross-links may have stayed with the incompletely digested and insoluble cell-wall residue. A more recent study demonstrated that a soluble HRGP from *Arabidopsis thaliana* cell culture that could be purified (extension AtEXT3) was competent to form a variety of tyrosine-tyrosine cross-links, including isodityrosines, when incubated *in vitro* with extension peroxidase.<sup>28</sup> Val-Tyr-Lys motifs have also been proposed as putative intermolecular cross-link sites on the basis of the ability of extracted soluble extensins to form cross-links *in vitro* in the presence of a purified peroxidase.<sup>17,29</sup> Although important for providing evidence that such cross-links can form and be detected, we reserve caution in extending the relevance of cross-links formed by purified protein *in vitro* to the likelihood of the same type of cross-links being formed within the organized and more complex cell-wall environment.

The possible conformations of an intramolecular Tyr<sub>1</sub>-Tyr<sub>3</sub> cross-linked pair of a YKY motif are restricted. A truly intermolecular Tyr-Tyr cross-link or a cross-link formed between two tyrosines distant in sequence, but still within the same polypeptide chain, can be accommodated by alternate conformations, as illustrated in Figure 3. A Tyr<sub>1</sub>-Tyr<sub>3</sub> pair results in a rigid structure (Figure 3, top left), whereas an interchain tyrosine cross-link is much less constrained (Figure 3, top right). An interchain cross-link is interpreted here to refer to two possibilities: (i) an intermolecular cross-link between two different proteins, i.e., two separate polypeptide chains, or (ii) an

(23) McDowell, L. M.; Schmidt, A.; Cohen, E. R.; Studelska, D. R.; Schaefer, J. *J. Mol. Biol.* **1996**, *256*, 160–171.

(24) Gullion, T.; Schaefer, J. *Adv. Magn. Reson.* **1989**, *13*, 57–83.

(25) Schaefer, J.; Stejskal, E. O.; McKay, R. A.; Dixon, T. *Macromolecules* **1984**, *17*, 1479–1489.

(26) Epstein, L.; Lamport, D. T. A. *Phytochemistry* **1984**, *23*, 1241–1246.

(27) Fry, S. C. *Annu. Rev. Plant Physiol.* **1986**, *37*, 165–186.

(28) Cannon, M. C.; Terneus, K.; Hall, Q.; Tan, L.; Wang, Y. M.; Wegenhart, B. L.; Chen, L. W.; Lamport, D. T. A.; Chen, Y. N.; Kieliszewski, M. J. *Proc. Natl. Acad. Sci. U.S.A.* **2008**, *105*, 2226–2231.

(29) Schnabelrauch, L. S.; Kieliszewski, M.; Upham, B. L.; Alizadeh, H.; Lamport, D. T. A. *Plant J.* **1996**, *9*, 477–489.

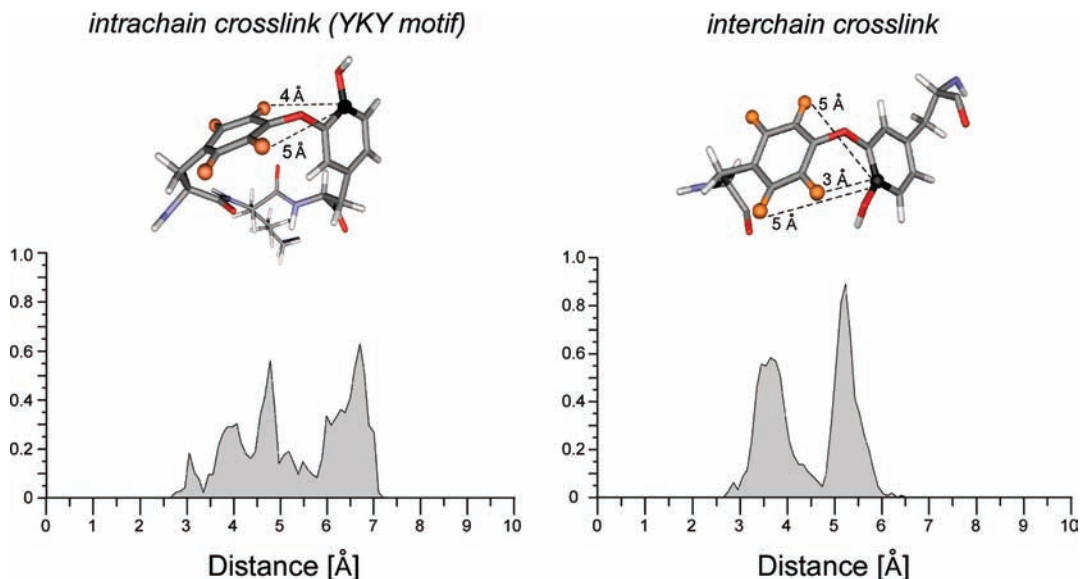


**Figure 3.** Molecular models (top) and distance distributions (bottom) of intra- and interchain isodityrosine. The intrachain energy-minimized peptide sequence (top left) was TPVYKYKSPPPP. Only the YKY segment is shown for clarity. The interchain cross-link (top right) was formed between two peptide chains of the sequence TPVYKYKSPPPP, where the first tyrosine of each sequence is participating in the interchain cross-link.

intramolecular cross-link between distant polypeptide stretches within the same protein.

Interchain cross-links between different polypeptide chains clearly could account for the gradual insolubility of the cell wall after assembly. Cross-links formed between tyrosines within the same polypeptide chain, but distant in sequence, could also yield the observed insolubility, especially because many cell-wall proteins are glycosylated and are thought to entangle in the cellulosic framework of the wall. If the polypeptide chain is entangled in the mesh and two distant segments approach each other to form a cross-link around cellulose fibrils, for example, mobility would be restricted and a strong, insoluble, yet flexible network would result. Such a self-assembly phenomenon could result in topologies akin to Borromean links.<sup>30</sup>

The distributions of distances from the *ring-4*-<sup>13</sup>C of one tyrosine to the <sup>2</sup>H labels of the cross-linked tyrosine differ between the two model structures (Figure 3, bottom). For an intrachain Tyr<sub>1</sub>–Tyr<sub>3</sub> cross-link, almost all the <sup>13</sup>C–<sup>2</sup>H distances are 4 Å or greater. Experimentally, the <sup>13</sup>C{<sup>2</sup>H} REDOR results for 48T<sub>r</sub> (Figure 2) are sensitive to the proximity of the nearest <sup>2</sup>H label, those within 4 Å. To support intrachain cross-links and the distribution of distances in Figure 3 (bottom left), we calculate that the dephasing could not be greater than about 15% at 48T<sub>r</sub>. However, the high probability of distances centered around 3.5 Å for the interchain conformation (Figure 3, bottom right) is consistent with 35% dephasing at 48T<sub>r</sub>. The observed REDOR dephasing is 20% (40% scaled, see above) at 48T<sub>r</sub>. Therefore, we conclude that the dominant number of isodityrosine cross-links are formed between tyrosines that are distant in sequence.

**Additional Constraints for the Tyrosine Chemical Environment from <sup>13</sup>C{<sup>15</sup>N} REDOR.** <sup>13</sup>C{<sup>15</sup>N} REDOR measurements were performed to probe a selected nitrogen environment near <sup>13</sup>C-labeled tyrosine. Possible <sup>15</sup>N dephasing can arise from the incorporated L-[ε-<sup>15</sup>N,6-<sup>13</sup>C]Lys and L-[<sup>15</sup>N]Pro amino acid labels. The ΔS spectrum identifies contact of the 155 ppm tyrosine <sup>13</sup>C label with nitrogen—either proline backbone

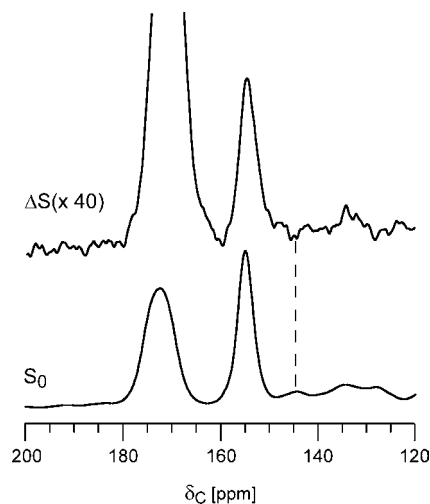


**Figure 4.** 125 MHz <sup>13</sup>C{<sup>15</sup>N} 64T<sub>r</sub> REDOR spectra of labeled cell walls. Some tyrosine carbons (155 ppm) are in proximity to lysine or proline <sup>15</sup>N labels ( $\Delta S/S_0 = 0.028$ ). There is no contact between the isodityrosine carbon (145 ppm) and <sup>15</sup>N labels (dotted line). Acquisition was at 125 MHz for <sup>13</sup>C, with spinning at 7143 Hz, a 1.5 s recycle delay, and 962 000 scans.

nitrogens or, more likely, lysine side-chain nitrogens—with a  $\Delta S/S_0$  of 2.8% (Figure 4). Similar contact for the diphenolic tyrosyl carbon to nitrogen would yield an observed  $\Delta S$  spectrum that is twice as large as the noise/baseline. However, no  $\Delta S$  is observed for the 145 ppm diphenolic carbon (Figure 4, dotted line). Therefore, the packing environment near the isodityrosine cross-link differs from that of the average tyrosine.

The lack of <sup>13</sup>C{<sup>15</sup>N} coupling between the diphenolic carbon and labeled lysine or labeled proline provides a molecular restraint to incorporate as we generate improved models of cell-wall architecture. We offer the possibility that the common occurrence of lysine–tyrosine neighbors, as in the YKY or VYK motifs, permits incidental lysine–tyrosine side-chain contact when tyrosines are not cross-linked. However, when tyrosines are engaged in cross-links, the lysine side chain is sterically occluded from extending in the same direction as a neighboring tyrosine side chain.

(30) Siegel, J. S. *Science* **2004**, *304*, 1256–1258.

Di-isodityrosine is a tetramer of tyrosine that has been observed after *in vitro* incubation of purified extensin analogues with an extensin peroxidase and peroxide.<sup>28</sup> As stated earlier, we think it is important to reserve caution in extending the detection of di-isodityrosine in this type of purified protein model system after incubation with a purified peroxidase to rendering implications for cell-wall assembly *in vivo*. Certainly, the intensities of the 155 and 145 ppm peaks expected for the mix of tyrosine and tyrosine cross-links observed *in vitro*<sup>28</sup> (a ratio of 2) do not match those observed *in situ* (a ratio of 7, Figure 2). In addition, the nature of protein steric constraints and allowable side-chain conformations (see Figure 3) decreases our enthusiasm for a model that includes a high density of di-isodityrosine, although future modeling and additional experimental studies *in situ* are needed to address this question quantitatively.

**$N\{^{13}C\}$  REDOR of L-[ $\epsilon$ - $^{15}N$ ,6- $^{13}C$ ]Lysine-Labeled, [ $^{15}N$ ]-Depleted Cell Walls.** Lysines are used extensively in the formation of cross-links in bacterial cell walls.<sup>31–33</sup> To explore the possibility that lysine side chains participate in plant cell-wall cross-links, we prepared a cell-wall sample from whole cells grown for two generations in the presence of L-[ $\epsilon$ - $^{15}N$ ,6- $^{13}C$ ]lysine and  $^{15}N$ -depleted ammonium nitrate and potassium nitrate. The ammonium nitrate  $^{15}N$  isotopic concentration (measured by mass spectrometry) was 0.003%, a depletion of a factor of 100 from natural-abundance levels.

The  $^{15}N\{^{13}C\}$  REDOR full-echo ( $S_0$ ) spectrum of the cell walls shows a ratio of integrated amine-to-amide intensities of approximately 42 (Figure 5, bottom two spectra). Assuming that lysine represents 5% of all cell-wall residues, that all of the lysines are  $^{15}N$ -labeled, and that all of the peptide nitrogens are at natural abundance, the expected amine-to-amide ratio is 17 ( $5 \times 0.99/95 \times 0.003$ ). Thus, the  $^{15}N$  depletion of ammonium nitrate has reduced the  $^{15}N$  isotopic abundance of the cell walls after two generations to 0.001, about a factor of 3. In addition to the starting level of  $^{15}N$ , the growing cells perhaps scavenged  $^{15}N$  from dead cells and debris in the growth media so that the reduction of isotopic enrichment was not the expected factor of 4 after two cell doublings.

The  $^{15}N\{^{13}C\}$  REDOR amide peak dephasing after eight rotor periods is small, barely above the noise (Figure 5, top). The dephasing for a directly bonded isopeptide  $^{13}C$ – $^{15}N$  pair (dipolar coupling of approximately 1200 Hz) is complete after  $8T_r$  with 5 kHz magic-angle spinning.<sup>20</sup> If we ignore peptide contributions to the 95 ppm dephasing for the moment, the ratio of  $\Delta S$  amide peak intensity centered at 95 ppm (Figure 5, dotted line) to  $\Delta S$  amine-peak intensity at 10 ppm is the fraction of cell-wall double-labeled lysyl residues that are chemically shifted and therefore part of putative isopeptide cross-links. This ratio is approximately 0.001; that is, one cross-link per 1000 lysines.

This cross-link value is, however, only an upper limit on the number of putative cross-links. Most of the 95 ppm  $S_0$  amide-peak intensity is due to the significant level of  $^{15}N$  in backbone peptide bonds (see above). We expect 2% dephasing of this signal from natural-abundance  $^{13}C$  in  $^{15}N$ – $^{13}C_\alpha$  and  $^{15}N$ – $^{13}C=O$

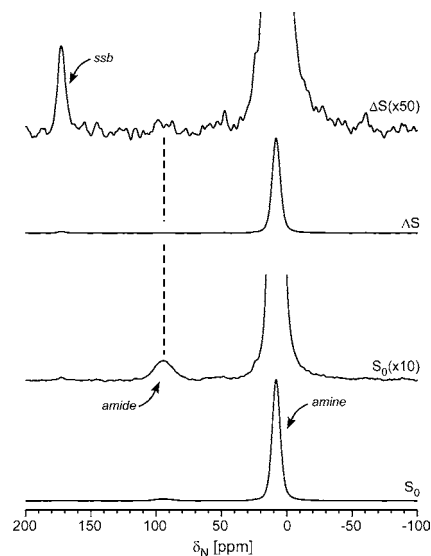


**Figure 5.** 30 MHz  $^{15}N\{^{13}C\}$   $8T_r$  REDOR spectra of soybean cell walls isolated from cells grown in culture on defined media that included L-[ $\epsilon$ - $^{15}N$ ,6- $^{13}C$ ]lysine and  $^{15}N$ -depleted ammonium nitrate as the only other nitrogen source. The full-echo spectrum ( $S_0$ ) is shown at the bottom of the figure, and the REDOR difference ( $\Delta S$ ) at the top. Dephasing for the  $^{15}N$ – $^{13}C$  amine pair at 10 ppm is 83%, consistent with dipolar coupling of approximately 900 Hz. The spectra are the result of the accumulation of 471 040 scans. Magic-angle spinning was at 5 kHz.

pairs. The observed 95 ppm  $\Delta S/S_0$  ratio is approximately 4%, but only half of the observed  $\Delta S$  could be due to isopeptide cross-links, with the other half due to peptide-bond dephasing by natural-abundance  $^{13}C$ . We conclude therefore that, if present, the number of cell-wall lysyls that are part of isopeptide cross-links can be no more than 1/2000 lysines in the cell wall sample. Lysyl secondary amine formation (50 ppm) is a possibility at the 1/1000 level.

## Conclusions

We have employed a novel combination of a biosynthetic isotope-labeling strategy in plant cells with site-specific REDOR NMR to detect isodityrosine cross-links in intact cell walls. The NMR measurements revealed that 25% of tyrosines in plant cell walls are engaged in cross-links, most of which are between tyrosines distant in polypeptide sequence or between proteins. Perhaps surprisingly, side chains of lysines are not significantly involved in covalent cross-linking in plant cell walls. The solid-state NMR determinations were made without the degradative measures and non-quantitative protein solubilization protocols that limit analyses by conventional methods. The combined labeling and NMR methodology introduced here can be extended to compare plant cell-wall cross-link densities as a function of environmental stress, such as drought, infection, or increased atmospheric  $CO_2$  concentrations, or as a function of genetic manipulations designed to simplify extraction of cell-wall material for biomass and biofuels.

**Acknowledgment.** This work was supported by the National Science Foundation under grant MCB-0613019 (J.S.). L.C. holds a Career Award at the Scientific Interface from the Burroughs Wellcome Fund.

JA104827K

(31) Wise, E. M., Jr.; Park, J. T. *Proc. Natl. Acad. Sci. U.S.A.* **1965**, *54*, 75–81.

(32) Strominger, J. L.; Ghuyssen, J. M. *Science* **1967**, *156*, 213–221.

(33) Ghuyssen, J. M. *Bacteriol. Rev.* **1968**, *32*, 425–464.